Longitudinally Misalignment-Insensitive Dual-Band Wireless Power and Data Transfer Systems for a Position Detection of Fast-Moving Vehicles

Wang-Sang Lee, *Senior Member, IEEE*, Sungsoo Park, *Member, IEEE*, Jae-Ho Lee, *Member, IEEE*, and Manos M. Tentzeris, *Fellow, IEEE*

***Abstract*— For position detection of moving vehicles using a wireless passive sensor placed in the traveling direction, a wireless power and data transfer (WPDT) system for supplying power to the sensor is required. Particularly, in the case of a high-speed vehicle with a compact sensor environment that is convenient for installation on railways or roadways, it is difficult to operate the sensor properly due to charging time and range limitations caused by the compact sensor size. In this paper, to improve a working zone of the compact sensor, this work presents a longitudinally misalignment-insensitive dual-band WPDT system with an extended working zone. The proposed system utilizes dual transmitting and receiving coils operating at different frequencies for achieving high isolation between the power and data links, which consists of a distributed antenna array with a gap between antenna elements for wireless power transfer at 27.1 MHz and an extended rectangular loop for data communications at 4.23 MHz. It achieves an extended working zone of approximately 112% at 0.25 m distance in comparison with a conventional system with dual square coils and achieves uniform received signals within a misalignment (up to 0.53 m).**

***Index Terms*— Compact wireless sensors, dual-band, fast-moving vehicle, longitudinally misalignment-insensitive, position detection, wireless power and data transfer (WPDT).**

I. Introduction

WITH an increase of electrical devices [e.g., consumer electronic devices, electric vehicles (EVs), etc.] used in everyday life, the energy industry is continuously expanding to meet an ever-growing energy consumption need. In order to remove the cumbersome usage of wiring to provide energy to devices or substantially minimizing electric shock hazards, the energy industry has been utilizing and developing wireless power and data transfer (WPDT) technologies to charge built-in batteries for electrical devices in recent years. WPDT devices can be used to transfer power (energy) and data (ID sensing, intelligent power control) from a source to a load without requiring a wired connection between them. In particular, modern digital devices, such as smartphones, tablets, and wearable devices for health monitoring, use batteries due to portability, and therefore, wireless charging is an attractive solution and becoming indispensable [1]. Recently, EVs have become popular for improving air quality through the reduction of harmful gases from vehicles. However, a long battery charging time and a short driving distance of EVs are demanding fundamental improvements. Dynamic wireless power transfer technology for EVs has attracted a lot of attention because it is one of the best ways to solve such problems [2].

WPDT technologies can be largely divided into two categories, radiative (far-field) and nonradiative (near-field) technologies [3]–[6]. The former is based on far-field radiation propagated between transmitting and receiving directional antennas for high efficiency in the long-range transmissions. However, since national regulatory authorities have limited the maximum radiation levels by considering the electromagnetic interference (EMI) on electric devices and the electromagnetic field (EMF) for human safety, it is difficult to commercialize far-field technologies for use in daily life [7], [8]. Depending on the coupling mechanisms through alternating electric and magnetic fields, near-field WPDT technologies can generally fall into two coupling categories: capacitive coupling and inductive coupling [9]. The capacitively and inductively coupled WPDT systems have a short operating distance, e.g., within less than a wavelength of the signal being transmitted. Moreover, the capacitive coupling causes a dielectric loss in a medium between the transmitting and receiving antennas [10].

Due to the increasing demand for the highly efficient WPDT applications, such as charging devices with spatial freedom, the magnetic resonance coupling using a high Q antenna, a sort of inductive coupling, has recently been attracting attention and focus [11], [12]. The working zones for the power transfer efficiency (PTE) and data communications are highly related to the product of the antenna Q-factor and the coupling coefficient (k) between the transmitting and receiving

Manuscript received October 3, 2018; revised March 7, 2019; accepted April 23, 2019. Date of publication May 20, 2019; date of current version August 12, 2019. This work was supported in part by the Gyeongsang National University Fund, for Professors on Sabbatical Leave, 2018, and in part by the Korean Government (MSIT) through the National Research Foundation of Korea under Grant NRF-2019R1C1C1008102. *(Corresponding author: Wang-Sang Lee.)*

W.-S. Lee is with the Department of Electronic Engineering, Engineering Research Institute (ERI), Gyeongsang National University (GNU), Jinju 52828, South Korea (e-mail: wsang@gnu.ac.kr).

S. Park and J.-H. Lee are with the Smart Electrical and Signaling Division, Advanced Railroad Technology Planning Department, Korea Railroad Research Institute (KRRI), Uiwang-si 16105, South Korea

M. M. Tentzeris is with the School of Electrical and Computer Engineering, Georgia Institute of Technology, Atlanta, GA 30332 USA.

Color versions of one or more of the figures in this paper are available online at http://ieeexplore.ieee.org.

Digital Object Identifier 10.1109/TAP.2019.2916697

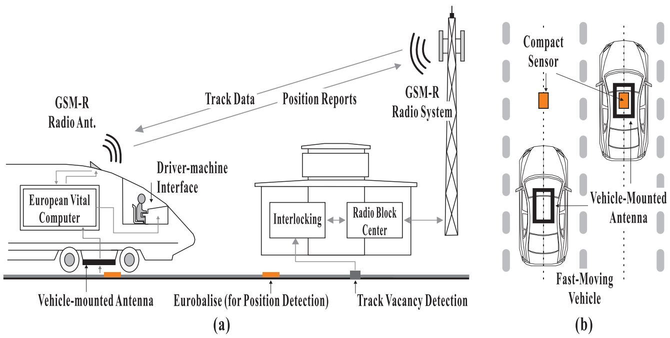

Fig. 1. Practical applications with longitudinal misalignment. (a) European signaling system ERTMS/ETCS Level 2. (b) Roadway vehicles with a compact sensor.

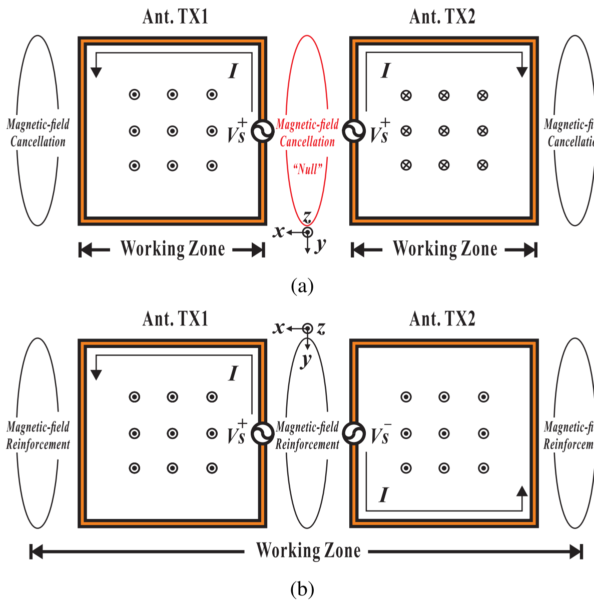

Fig. 2. Magnetic field cancellation and reinforcement principles with regard to the current direction between adjacent power transfer TX antennas (Ant. TX1 and Ant. TX2). (a) Opposite directions. (b) Same directions.

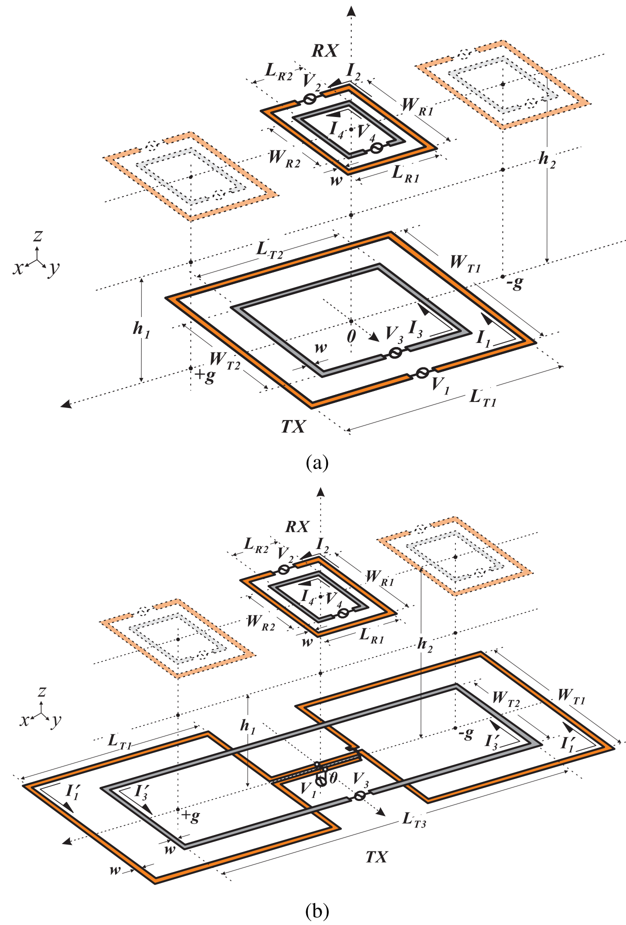

Fig. 3. Coil configurations of a WPDT system with loosely coupled compact sensors. (a) Conventional transmitting and receiving antenna structures. (b) Proposed misalignment-insensitive antenna structures.

antennas. To improve the PTE, the near-field WPDT systems require high Q resonant coil antennas using a low antenna loss and a high reactance, which is achieved by setting a high operating frequency (up to tens of MHz) [12], multiple turns [13], tilt angle variation [14], frequency tracking control [15], or an additional coil [16], [17]. The k depends on a mutual inductance (M) of which the main factors are related to the operating distance and the antenna alignments [18]. Although the antennas are placed at a short working distance, the PTE under a misalignment between transmitting and receiving antennas is very low due to the impedance mismatch [19]. In the case of dynamic wireless charging, the degraded PTE caused by longitudinal misalignment decreases the charging range [20]. Another typical example of degradation in WPDT system performance during misalignment is the railroad environment. Fig. 1(a) describes Eurobalises (or balises for short) acting as position markers in the European signaling system. The European Rail Traffic Management System/European Train Control System (ERTMS/ETCS) play an important role in the position detection of a high-speed train [21]. Generally, balises receive the telepowering signal generated by the vehicle-mounted antenna unit and transmit the position and control information to the vehicle using the telepowering signal at different frequency bands. Fig. 1(b) describes roadway vehicles moving along a track having a compact position detection sensor. As the vehicle passes the sensor in a short charging time, the working zone of the sensor depends on a longitudinal misalignment characteristic as well as a distance between the transmitting and receiving antennas. In particular, the miniaturization of the sensor in the high-speed vehicle significantly reduces the working zone.

To improve the PTE of the misaligned WPDT and solve the PTE degradation due to the impedance mismatching, several studies using multiple transmitting antennas [22], [24], [26], antiparallel resonant loops [25], metasurfaces [26], a dipole coil [27], adaptive impedance matching techniques [28], [29], or uniform field distributions [30] were proposed. In this paper, a near-field coupled dual-band WPDT system without any additional adaptive circuits using a longitudinally misalignment-improved loop array for telepowering and data communications to compact stand-alone wireless sensors is presented for consideration.

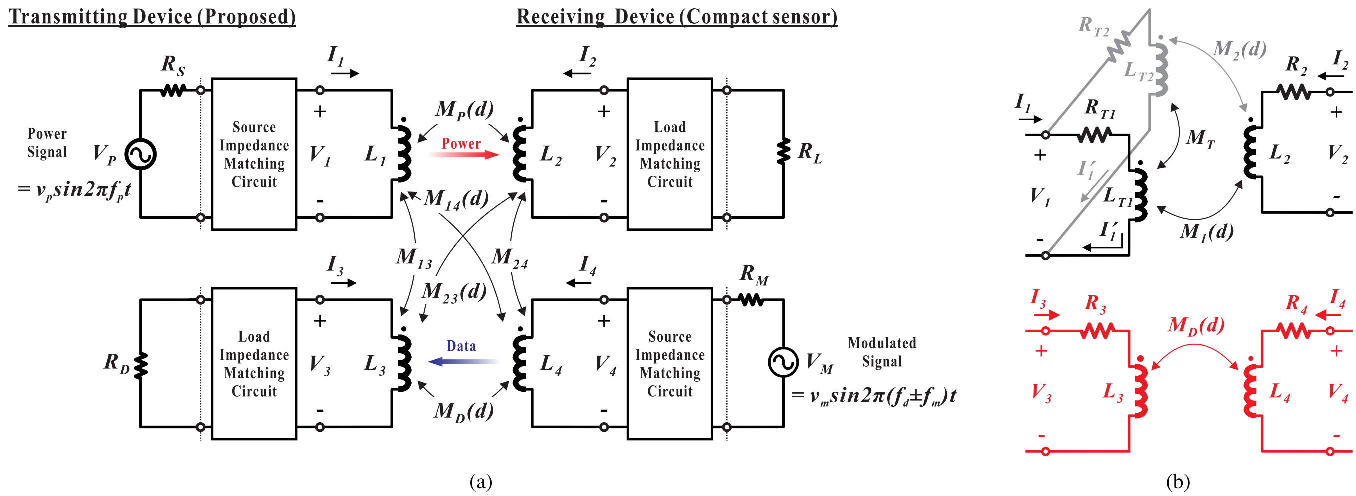

Fig. 4. Overall system configurations. (a) Block diagrams of a longitudinally misalignment-insensitive WPDT system for a loosely coupled compact wireless sensor. (b) Simplified equivalent circuits of proposed loosely coupled transmitting and receiving antenna configurations with a large air gap.

II. Operating Principles of the Proposed Misalignment-Insensitive WPDT System

This section covers the operating principles of the proposed misalignment-insensitive WPDT systems with dual-band dual coils with different frequencies (f_p for downlink power transfer and f_d for uplink data transfer). To achieve an extended working zone under the loosely coupled compact wireless sensors, a longitudinally misalignment-insensitive distributed coil array for power transfer and a single-turn rectangular loop coil for data communications are proposed. Fig. 2 shows the magnetic field cancellation and superposition principles with regard to the current direction between adjacent power transfer transmitting (TX) antennas. With regard to the current directions of the TX antennas, the magnetic field at the space between the antennas can be canceled or superposed in Fig. 2(a) and (b). For wide-range nonradiative wireless charging with an extended working zone, the power transfer TX antennas with the same counterclockwise current have been proposed. To prevent the noise coupling (in particular, the effect of harmonics) between the power and data links, the dual-band dual coils are configured in Fig. 3, and the f_d lower than the f_p has been determined. The conventional single-turn TX and RX coils in Fig. 3(a) have dual coil (power and data) structures, whereas the proposed coils in Fig. 3(b) consist of the TRX dual coil, such as a distributed TX array (power) and a high isolated rectangular RX loop (data), and the single-turn dual TRX coil (RX for power and TX for data). Fig. 4(a) shows the overall block diagram of a misalignment-insensitive WPDT system for a loosely coupled compact wireless sensor with power and data transfer single-turn coils. The power of the stand-alone sensor is wirelessly provided by the coupled circuit from a TX device. The modulated signal (data) from the sensor is generated and sent to the transmitter. Due to the different frequency bands (f_p and f_d) in the power and data transfer links, simplified equivalent circuits for the proposed TX and RX antenna configurations with a large air gap can be seen in Fig. 4(b).

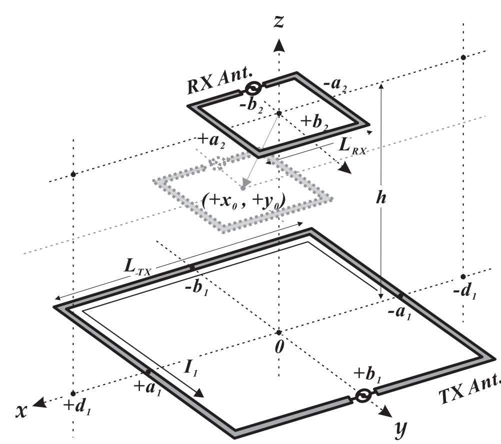

Fig. 5. Mutual inductance between two single loops with a misalignment.

III. Theoretical Analysis of a WPDT System and Its Design Considerations

A. Analysis of Mutual Inductance Between Two Loops

Using a Neumann formula, the mutual inductance (M_{ref} in conventional coils) between two single-turn rectangular loops with the offset (x_0, y_0) at the distance (h) in Fig. 5 can be calculated using

$$\begin{aligned} M_{\text{ref}}(x_0, y_0) &= \frac{\psi_2}{I_1} = \frac{\int_{S_2} \mathbf{B} \cdot d\hat{s}}{I_1} \\ &= \frac{\int_{S_2} \frac{\mu_0 I_1}{4\pi} \int_l \frac{\hat{l} \times \hat{a}_R}{R^2} dl \cdot d\hat{s}}{I_1} \\ &= \frac{\mu_0}{4\pi} \sum_{i=0}^{1} \sum_{j=0}^{1} \sum_{k=0}^{1} \sum_{l=0}^{1} (-1)^{l+k+j+i} \\ &\quad \cdot \begin{bmatrix} 2\sqrt{x_{kl}^2 + y_{ij}^2 + h^2} \\ -x_{kl} \ln\left(x_{kl} + \sqrt{x_{kl}^2 + y_{ij}^2 + h^2}\right) \\ -y_{ij} \ln\left(y_{ij} + \sqrt{x_{kl}^2 + y_{ij}^2 + h^2}\right) \end{bmatrix} \end{aligned} \tag{1}$$

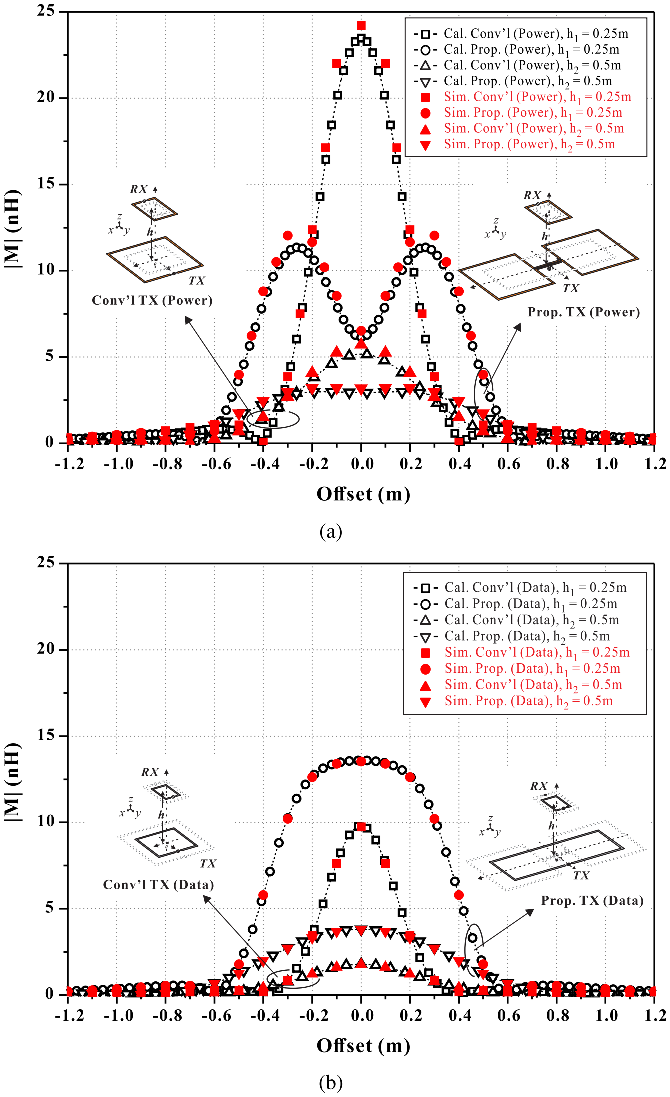

Fig. 6. Calculated and simulated mutual inductances for the conventional and proposed power and data transmitting antennas under a single-turn receiving coil with regard to the air gaps ($h_1 = 0.25$ m and $h_2 = 0.5$ m). (a) Downlink power transfer. (b) Uplink data transfer.

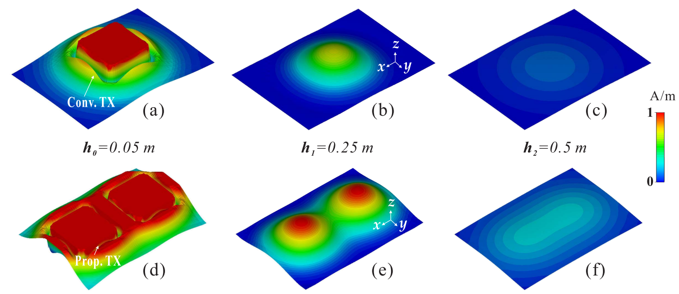

Fig. 7. Magnetic field distributions with regard to different air gaps (h) away from the TX antennas for power transfer.

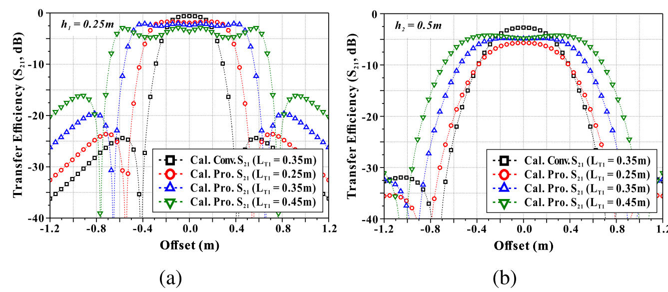

Fig. 8. PTE with regard to the offset between the transmitting and receiving antennas at different TX antenna lengths (L_{T1}). (a) $h_1 = 0.25$ m. (b) $h_2 = 0.5$ m.

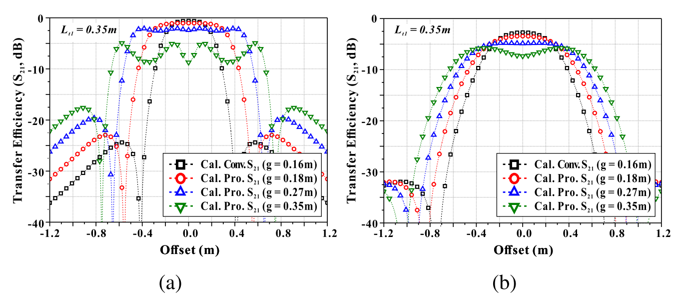

Fig. 9. PTE with regard to the offset between the transmitting and receiving antennas at different TX spacings (g). (a) $h_1 = 0.25$ m. (b) $h_2 = 0.5$ m.

where $x_{kl} = x_0 + (-1)^k L_{\mathrm{RX}}/2 + (-1)^l L_{\mathrm{TX}}/2$, $y_{ij} = y_0 + (-1)^i L_{\mathrm{RX}}/2 + (-1)^j L_{\mathrm{TX}}/2$, and μ_0 is the magnetic constant ($4\pi \times 10^{-7}$ H/m). When the proposed distributed antenna array which consists of two square loops separated by a gap distance (g) from the antenna center is deployed in the x-axis in Fig. 3(b), the mutual inductance (M_{pro}) which is represented by the superposition of (1) can be determined by

$$M_{\mathrm{pro}}(x_0, 0) = \sum_{i=0}^{1} \frac{M_{\mathrm{ref}}(x_0 + (-1)^i \cdot g, 0)}{2}. \tag{2}$$

Fig. 6 shows the calculated and simulated mutual inductances for conventional and proposed TX antennas under a single-turn RX antenna with regard to the operating distance (h) at power and data transfer links, respectively. When the antenna physical dimensions, such as the TX antenna side lengths ($L_{T1} = W_{T1} = 0.35$ m) for power transfer, the TX antenna side lengths ($L_{T2} = W_{T2} = 0.25$ m, $L_{T3} = 0.78$ m) for data communications, the gap distance ($g = 0.26$ m) between the center of the proposed TX array and the square antenna, the RX antenna side lengths ($L_{R1} = 0.25$ m, $W_{R1} = 0.14$ m) for power transfer, the RX antenna side lengths ($L_{R2} = 0.21$ m, $W_{R2} = 0.10$ m) for data communications, and the linewidth ($w = 0.01$ m) of the antenna, are determined, the calculated results based on (1) and (2) are in good agreement with the simulated results using a method of moment (MoM) solver of Microwave Office by Applied Wave Research (AWR) Corporation. As the air gap (h) in Fig. 6(a) increases, the uniform mutual inductance range is achieved. Compared to the conventional antennas, the proposed antennas have wide uniform mutual inductance within a large offset. In particular, the conventional antennas at zero-offset achieve a mutual inductance that has approximately five times larger than the proposed design. This means that the impedance mismatch within a misalignment in the proposed antennas cannot be generated, and the working zones of their WPDT systems have been extended.

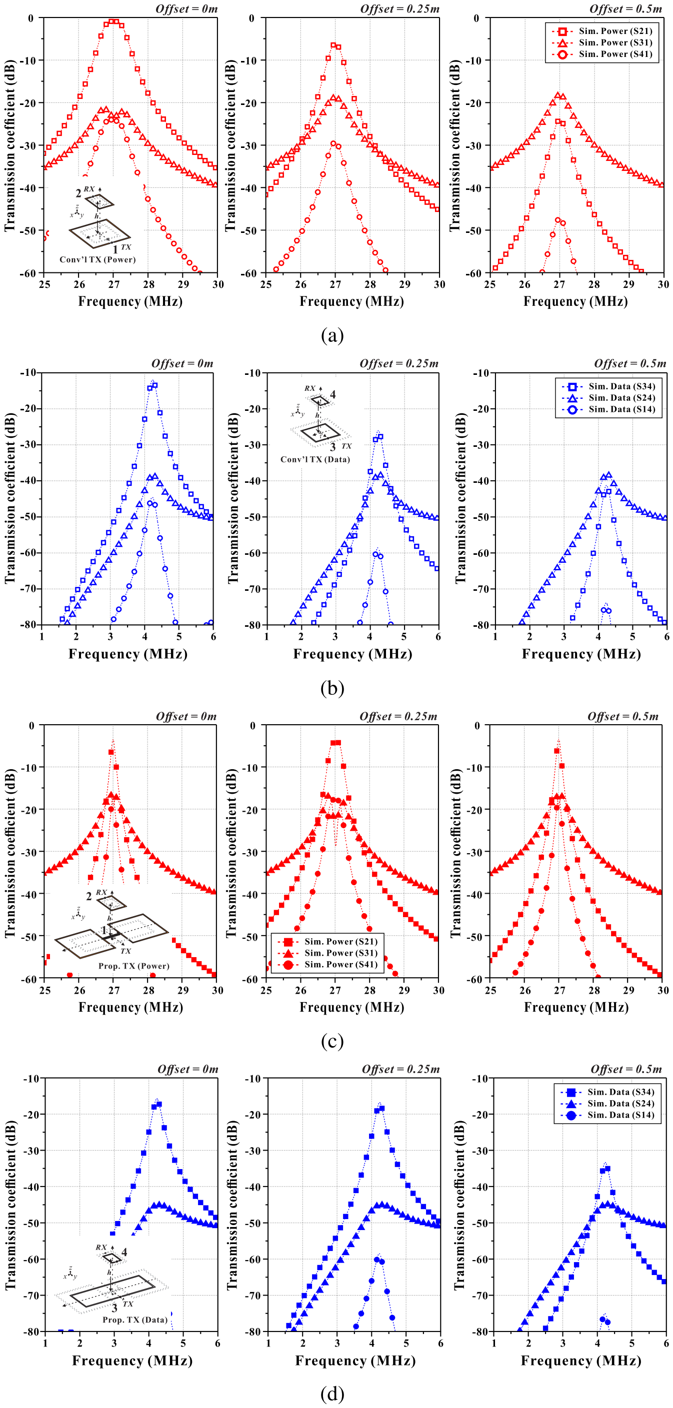

Fig. 10. Simulated transmission coefficients and isolations between the TX (conventional) and RX antennas regarding the operating frequency at different offsets for $h_1 = 0.25$ m. (a) Downlink power transfer at conventional coils. (b) Uplink data transfer at conventional coils. (c) Downlink power transfer at proposed coils. (d) Uplink data transfer at proposed coils.

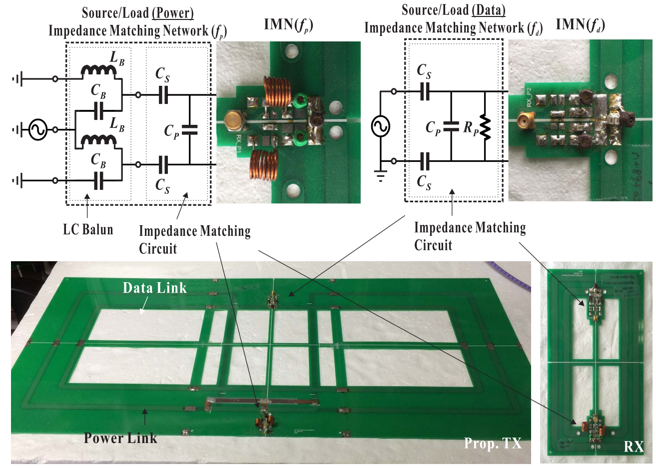

Fig. 11. Fabricated prototype and IMN schematics in the power and data links.

TABLE I

LINK SPECIFICATIONS AND COMPARISON OF DESIGN PARAMETERS BETWEEN ANTENNA LINKS

Specifications		Power Transfer	Data Commu.
Operating Freq. f_p, f_d, MHz		27.1	4.23
Min. Operating Distance h, m		0.25	
Min. Offset Distance, m		0.50	
Max. TX Ant. Size $L \times W$, m^2		N/A $\times$ 1.00	N/A $\times$ 1.00
Max. RX Ant. Size $L \times W$, m^2		0.25 $\times$ 0.15	0.25 $\times$ 0.15
Parameter		Conv'l TX / RX	Prop. TX / RX
Power Transfer	Unloaded Q	264 / 314	151 / 314
	LC Balun L_B, nH	417 / 417	
	LC Balun C_B, pF	83 / 83	
	Series Cap. C_s, pF	11.5 / 18.9	12.1 / 5.8
	Parallel Cap. C_p, pF	25.2 / 66.9	37.1 / 73.2
Data Commu.	Unloaded Q	235 / 122	154 / 122
	Series Cap. C_s', pF	458 / 424	412 / 391
	Parallel Cap. C_p', pF	3416 / 1714	3426 / 653
	Parallel Res. R_p, Ω	510 / 510	

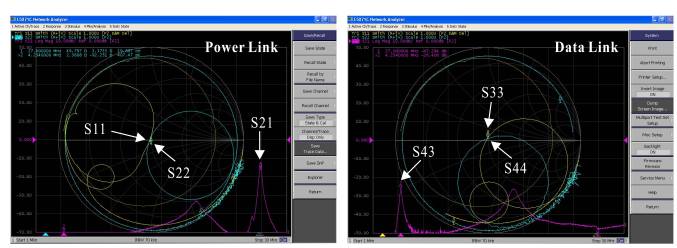

Fig. 12. Measured input impedance on Smith chart at the distance (h_2).

B. Transfer Efficiency and Isolation Analysis of Power and Data Transfer Links

To achieve highly efficient WPDT in loosely coupled circuits, there must be a simultaneous conjugate impedance matching networks (IMNs) at the source and the loads required for this are shown in Fig. 4(a). Generally, the overall PTE from the transmitter to the receiver in WPDT systems depends on the link transfer efficiency regarding the coupled circuits. The link efficiency under the impedance matching can be determined by

$$|S_{21}(d)|^2_{f_0} = \frac{1}{\left(\sqrt{1 + Q_M^{-2}(d)} + \sqrt{Q_M^{-2}(d)}\,\right)^2} \tag{3}$$

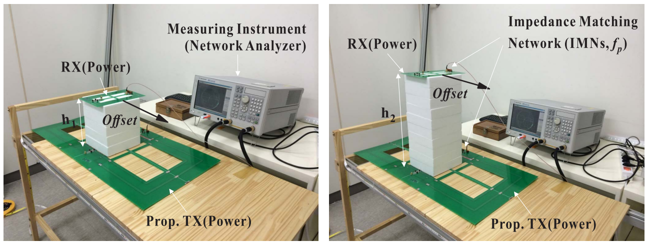

(a)

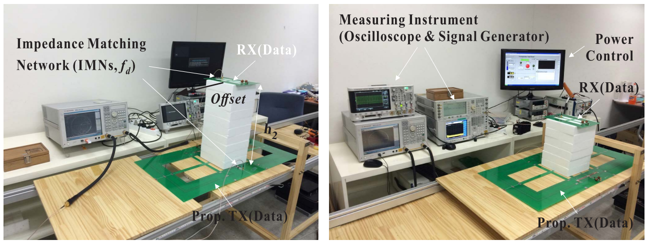

(b)

Fig. 13. Measurement setups of transfer efficiency (S_{21}) with regard to a misalignment at the operating distance (h_1 and h_2) using measuring instruments. (a) Power transfer link. (b) Data communications link.

where $Q^2_{M,f_0}(d) = \omega_0^2\ M^2(d)/(R_{\rm TX} R_{\rm RX}) = k^2 Q_{\rm TX} Q_{\rm RX}$, and the R and Q are the equivalent series resistances (ESRs) and unloaded Q-factors in the TX and RX coils, respectively [19]. According to different M at the coupled circuit conditions, such as the multiple receiver variable operating distance, or misalignments, the impedance mismatch degrades the PTE. By additionally inserting adaptive circuits, the degraded PTE can be improved [28]. However, in this case, the WPDT system structure becomes complicated, and a loss due to the additional circuits is generated. In particular, when the size of the RX coil is reduced, and the TX and RX coils are misaligned, the M and the working distance are decreased due to the reduction of the loop area, and its PTE is drastically decreased.

Using a 3-D full-wave electromagnetic simulation software (Microwave Studio 2018 by CST), Fig. 7 describes the magnetic field distributions with regard to different air gaps. The magnetic field distributions of the proposed TX antenna array for power transfer within a misalignment is much more uniform than that of a conventional TX antenna. Compared to the PTEs in conventional coils, Figs. 8 and 9 show that the PTEs of the proposed dual coil antennas at $h_1 = 0.25$ m and $h_2 = 0.5$ m are analyzed by altering the different TX antenna side lengths (L_{T1}) and TX gap distances (g), respectively. The proposed distributed antenna array achieves an extended working zone. In Fig. 9(a), when the g is getting large from 0.18 to 0.35 m, the nulls which drastically decrease the PTE are generated within the working zone.

In order to describe the signal coupling at power and data transfer links, Fig. 10 shows the simulated transmission coefficients and isolations between the TX (conventional or proposed coils) and RX antennas with regard to the operating frequency at the longitudinal misalignments for $h_1 = 0.25$ m. Due to the different frequency bands ($f_p = 27.1$ mHz for power transfer, $f_d = 4.23$ mHz for data transfer), the signal isolations at power and data transfer links, regardless of

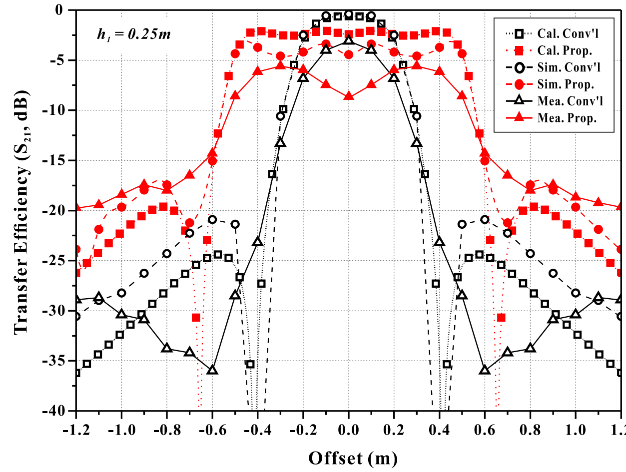

(a)

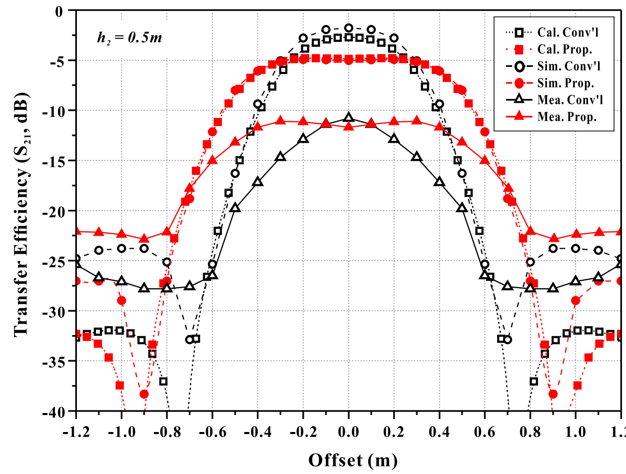

(b)

Fig. 14. Power transfer efficiency comparisons among the calculated, simulated, and measured results regarding the offset between the transmitting (conventional or proposed) and receiving antennas at different operating distances (h). (a) $h_1 = 0.25$ m. (b) $h_2 = 0.5$ m.

the offset distances, maintains approximately 20 and 40 dB, respectively. On the other hand, the larger the offset distances are, the lower is the PTE in the conventional coils. However, the proposed coils achieve the uniform PTE within a misalignment distance (up to 0.5 m).

IV. Experimental Verifications

To validate the operating principles and a longitudinally misalignment-insensitive characteristic of the proposed near-field coupled WPDT systems with an extended working zone for compact wireless sensors, the proposed coils having a distributed antenna array were designed and fabricated on a double-sided FR-4 printed circuit board (PCB) substrate, which has a substrate thickness of 1 mm, a dielectric constant (ϵ_r) of 4.5, and a copper thickness (t) of 18 μm. Applying for longitudinally misalignment-insensitive WPDT in the near-field, the power transfer frequency was set to 27.1 MHz by considering the air-gap requirements for Eurobalise in order to serve as a solid basis for the interoperability with any ERTMS/ETCS compliant on-board equipment [31].

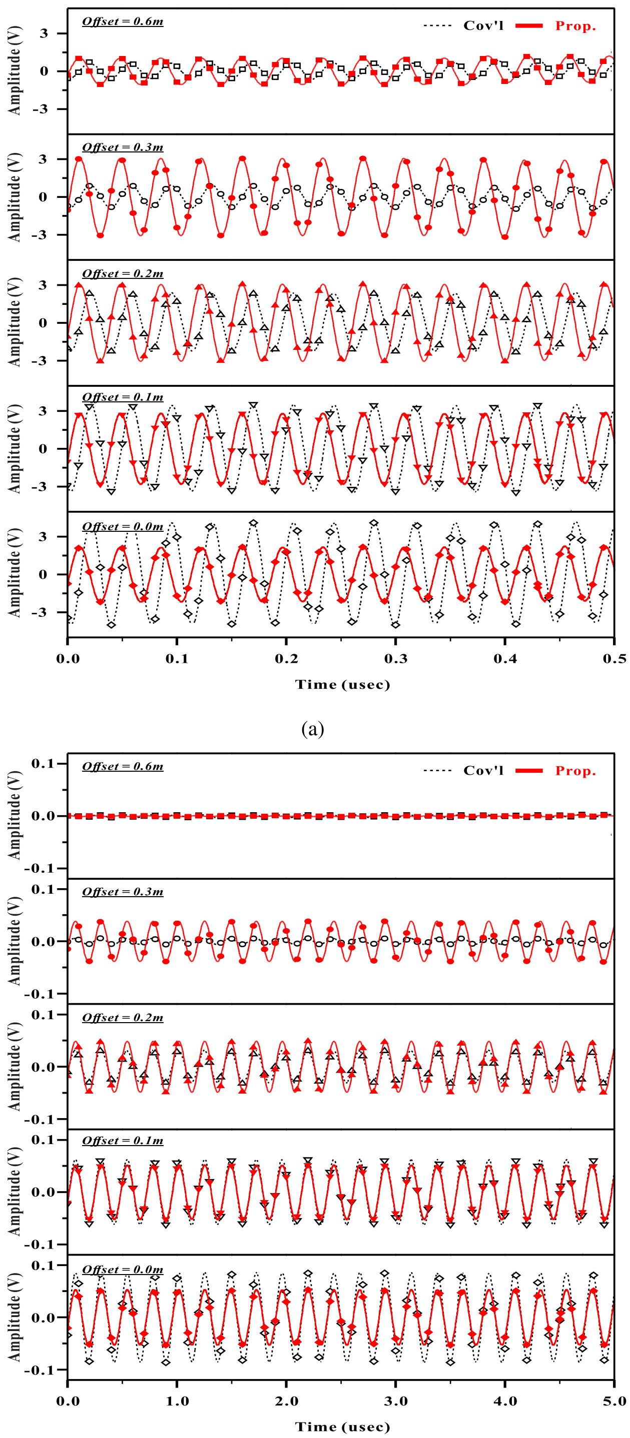

(a)

(b)

Fig. 15. Signal waveforms between the transmitting and receiving antennas regarding different offsets (0 m ∼ 0.6 m) distances at $h_1 = 0.25$ m. (a) Power transfer link (TX input power: 1 W at 27.1 MHz). (b) Data communications link (TX input power: 1 mW at 4.23 MHz).

Fig. 11 shows the IMN schematics and their implementations in the power and data transfer links. At 27.1 MHz for downlink power transfer, the IMN consists of LC balun (L_B and C_B) for impedance transformation and the balanced to unbalanced conversion, and series and parallel capacitors (C_s and C_p) for impedance matching. Unlike the power transfer frequency, the uplink data transfer frequency was set to 4.23 MHz, and the IMN in the link consists of series and parallel capacitors (C_s' and C_p') for impedance matching and a damping resistor (R_p) to control the Q for data transfer. When the RX coil was located at the center position of the TX coil, the impedance matching was done at the operating distance. Table I summarizes the link specifications and comparison of design parameters between antenna links for power transfer and data communications.

TABLE II

RECEIVED PEAK-TO-PEAK SIGNALS AT POWER AND DATA LINKS

Offset (m)	Power transfer link			
	Peak-to-Peak (V)		Normalized results[1]	
	Conv'l TX	Prop. TX	Conv'l TX	Prop. TX
0	8.10	4.74	1.62	0.95
0.1	6.51	5.79	1.30	1.16
0.2	3.92	6.51	0.78	1.30
0.3	1.53	6.51	0.31	1.30
0.4	1.45	6.67	0.29	1.33
0.5	1.42	4.98	0.28	1.00
0.6	1.41	2.01	0.28	0.40
0.9	1.40	0.56	0.28	0.11
1.2	1.40	0.56	0.28	0.11
Offset (m)	**Data communications link**			
	Peak-to-Peak (V)		Normalized results[1]	
	Conv'l TX	Prop. TX	Conv'l TX	Prop. TX
0	173	106	8.65	5.30
0.1	129	106	6.45	5.30
0.2	64	100	3.20	5.00
0.3	11.7	79	0.59	3.95
0.4	9.9	45	0.50	2.25
0.5	8.2	18	0.41	0.90
0.6	6	2.8	0.30	0.14
0.9	3.6	5	0.18	0.25
1.2	2.4	3.2	0.12	0.16

[1] Based on 5V for power link and 20mV for data link

Figs. 12 and 13 show the measured input impedance on Smith chart at the distance (h_2) and the measurement setups of transfer efficiency (S_{21}) with the misalignments at operating distance ($h_1 = 0.25$ m and $h_2 = 0.5$ m) in power and data transfer links using measuring instruments. To measure the PTE between the TX (conventional or proposed) and RX coils, a two-port vector network analyzer (E5071C, Keysight Technologies) was utilized. Transfer efficiency comparisons among the calculated, simulated, and measured results regarding the offset between the TX (conventional or proposed) and receiving antennas at the distance (h) are shown in Fig. 14. Due to the PCB implementation of the TX and RX coils or the loss of the passive RLC components, the experimental results were slightly degraded. However, the overall results against longitudinal misalignments, were consistent with the theoretical results, and were obtained for the operating distance. Based on the −10 dB of the transfer efficiency, the proposed near-field power transfer link has a longitudinally misalignment-improvement of approximately 112% compared to the conventional link at h_1 in Fig. 14(a). For the demonstration of power and data transfer characteristics in the time domain, the TX coils were applied to the signal source with 1 W at 27.1 MHz for power transfer link or 1 mW at 4.23 MHz for data communications link, respectively.

Fig. 15 shows the time-domain signal waveforms between the transmitting (conventional or proposed) and receiving antennas regarding the different offset distances at the power or data transfer links. Table II represents the received peak-to-peak signals under the conventional or proposed TX coil with regard to the offset (up to 1.2 m) at $h_1 = 0.25$ m. Within the longitudinal misalignment up to 0.53 m, the power and data received signals in the conventional TX and RX coils were significantly decreased. However, the PTE of the proposed near-field coupled WPDT system at the $h_1 = 0.25$ m achieves approximately 10% and the received power and data signal levels remain constant.

V. Conclusion

This paper has presented and demonstrated a near-field coupled misalignment-insensitive WPDT systems for telepowering and data communications to compact wireless sensors. Using dual-band dual coils which consist of a proposed distributed antenna array for power transfer and an extended rectangular loop for data communications without additional circuits and algorithms for improving a impedance mismatching problem, the proposed WPDT system can achieve uniform power and data transfer characteristics at an extended working zone (up to 0.5 m of longitudinal misalignment). The proposed misalignment-insensitive system can be utilized for the detection and precise location of high-speed vehicles by detecting the compact receiving devices in a short time. Moreover, it is helpful to improve the PTE of portable WPDT applications as well as stationary or dynamic wireless charging applications in the residential garages, public parkings, or highway environments.

References

[1] X. Lu, P. Wang, D. Niyato, D. I. Kim, and Z. Han, "Wireless charging technologies: Fundamentals, standards, and network applications," *IEEE Commun. Surveys Tuts.*, vol. 18, no. 2, pp. 1413–1452, 2nd Quart., 2016.

[2] S. Li and C. C. Mi, "Wireless power transfer for electric vehicle applications," *IEEE J. Emerg. Sel. Topics Power Electron.*, vol. 3, no. 1, pp. 4–17, Mar. 2015.

[3] B. Strassner and K. Chang, "Microwave power transmission: Historical milestones and system components," *Proc. IEEE*, vol. 101, no. 6, pp. 1379–1396, Jun. 2013.

[4] M. Ettorre, W. A. Alomar, and A. Grbic, "2-D Van Atta array of wideband, wideangle slots for radiative wireless power transfer systems," *IEEE Trans. Antennas Propag.*, vol. 66, no. 9, pp. 4577–4585, Sep. 2018.

[5] A. A. Eteng, S. K. A. Rahim, and C. Y. Leow, "Wireless nonradiative energy transfer: Antenna performance enhancement techniques," *IEEE Antennas Propag. Mag.*, vol. 57, no. 3, pp. 16–22, Jun. 2015.

[6] Y. Lim, H.-S. Ahn, and J. Park, "Analysis of antenna structure for energy beamforming in wireless power transfer," *IEEE Trans. Antennas Propag.*, vol. 65, no. 11, pp. 6085–6094, Nov. 2017.

[7] W. S. Lee, K. S. Oh, and J. W. Yu, "Field analysis and measurement of antiparallel resonant loop for wireless charging," *IEEE Antennas Wireless Propag. Lett.*, vol. 14, pp. 1459–1462, 2015.

[8] S. Y. R. Hui, W. Zhong, and C. K. Lee, "A critical review of recent progress in mid-range wireless power transfer," *IEEE Trans. Power Electron.*, vol. 29, no. 9, pp. 4500–4511, Sep. 2014.

[9] J. Dai and D. C. Ludois, "A survey of wireless power transfer and a critical comparison of inductive and capacitive coupling for small gap applications," *IEEE Trans. Power Electron.*, vol. 30, no. 11, pp. 6017–6029, Nov. 2015.

[10] L. Huang and A. P. Hu, "Defining the mutual coupling of capacitive power transfer for wireless power transfer," *Electron. Lett.*, vol. 51, no. 22, pp. 1806–1807, Oct. 2015.

[11] A. Kurs, A. Karalis, R. Moffatt, J. D. Joannopoulos, P. Fisher, and M. Soljačić, "Wireless power transfer via strongly coupled magnetic resonances," *Science*, vol. 317, pp. 83–86, Jul. 2007.

[12] A. P. Sample, D. T. Meyer, and J. R. Smith, "Analysis, experimental results, and range adaptation of magnetically coupled resonators for wireless power transfer," *IEEE Trans. Ind. Electron.*, vol. 58, no. 2, pp. 544–554, Feb. 2011.

[13] X. Ju, L. Dong, X. Huang, and X. Liao, "Switching technique for inductive power transfer at high-Q regimes," *IEEE Trans. Ind. Electron.*, vol. 62, no. 4, pp. 2164–2173, Apr. 2015.

[14] W. Huang and H. Ku, "Analysis and optimization of wireless power transfer efficiency considering the tilt angle of a coil," *J. Electromagn. Eng. Sci.*, vol. 18, no. 1, pp. 13–19, Jan. 2018.

[15] S. Aldhaher, P. C.-K. Luk, and J. F. Whidborne, "Electronic tuning of misaligned coils in wireless power transfer systems," *IEEE Trans. Power Electron.*, vol. 29, no. 11, pp. 5975–5982, Nov. 2014.

[16] J. Lee, Y. Lim, H. Ahn, J.-D. Yu, and S.-O. Lim, "Impedance-matched wireless power transfer systems using an arbitrary number of coils with flexible coil positioning," *IEEE Antennas Wireless Propag. Lett.*, vol. 13, pp. 1207–1210, 2014.

[17] S. Mao, J. Zhang, K. Song, G. Wei, and C. Zhu, "Wireless power transfer using a field-enhancing coil and a small-sized receiver with low coupling coefficient," *IET Power Electron.*, vol. 9, no. 7, pp. 1546–1552, Jun. 2016.

[18] D. Liu, H. Hu, and S. V. Georgakopoulos, "Misalignment sensitivity of strongly coupled wireless power transfer systems," *IEEE Trans. Power Electron.*, vol. 32, no. 7, pp. 5509–5519, Jul. 2017.

[19] W.-S. Lee, K.-S. Oh, and J.-W. Yu, "Distance-insensitive wireless power transfer and near-field communication using a current-controlled loop with a loaded capacitance," *IEEE Trans. Antennas Propag.*, vol. 62, no. 2, pp. 936–940, Feb. 2014.

[20] T. Fujita, T. Yasuda, and H. Akagi, "A dynamic wireless power transfer system applicable to a stationary system," *IEEE Trans. Ind. Appl.*, vol. 53, no. 4, pp. 3748–3757, Jul./Aug. 2017.

[21] S. Dhahbi, A. Abbas-Turki, S. Hayat, and A. El Moudni, "Study of the high-speed trains positioning system: European signaling system ERTMS/ETCS," in *Proc. 4th Int. Conf. Logistics*, May/Jun. 2011, pp. 468–473.

[22] K. Lee, Z. Pantic, and S. M. Lukic, "Reflexive field containment in dynamic inductive power transfer systems," *IEEE Trans. Power Electron.*, vol. 29, no. 9, pp. 4592–4602, Sep. 2014.

[23] H.-D. Lang, A. Ludwig, and C. D. Sarris, "Convex optimization of wireless power transfer systems with multiple transmitters," *IEEE Trans. Antennas Propag.*, vol. 62, no. 9, pp. 4623–4636, Sep. 2014.

[24] R. Johari, J. V. Krogmeier, and D. J. Love, "Analysis and practical considerations in implementing multiple transmitters for wireless power transfer via coupled magnetic resonance," *IEEE Trans. Ind. Electron.*, vol. 61, no. 4, pp. 1774–1783, Apr. 2014.

[25] W.-S. Lee, W.-I. Son, K.-S. Oh, and J.-W. Yu, "Contactless energy transfer systems using antiparallel resonant loops," *IEEE Trans. Ind. Electron.*, vol. 60, no. 1, pp. 350–359, Jan. 2013.

[26] H.-D. Lang and C. D. Sarris, "Optimization of wireless power transfer systems enhanced by passive elements and metasurfaces," *IEEE Trans. Antennas Propag.*, vol. 65, no. 10, pp. 5462–5474, Oct. 2017.

[27] B. H. Choi, V. X. Thai, E. S. Lee, J. H. Kim, and C. T. Rim, "Dipole-coil-based wide-range inductive power transfer systems for wireless sensors," *IEEE Trans. Ind. Electron.*, vol. 63, no. 5, pp. 3158–3167, May 2016.

[28] Y.-J. Kim, D. Ha, W. J. Chappell, and P. P. Irazoqui, "Selective wireless power transfer for smart power distribution in a miniature-sized multiple-receiver system," *IEEE Trans. Ind. Electron.*, vol. 63, no. 3, pp. 1853–1862, Mar. 2016.

[29] S. G. Lee, H. Hoang, Y. H. Choi, and F. Bien, "Efficiency improvement for magnetic resonance based wireless power transfer with axial-misalignment," *Electron. Lett.*, vol. 48, no. 6, pp. 339–340, Mar. 2012.

[30] B. M. Badr, R. Somogyi-Gsizmazia, K. R. Delaney, and N. Dechev, "Wireless power transfer for telemetric devices with variable orientation, for small rodent behavior monitoring," *IEEE Sensors J.*, vol. 15, no. 4, pp. 2144–2156, Apr. 2015.

[31] *UNISIG FFFIS for Eurobalise Subset-036*, Eurobalise Standard SUBSET-036, ERTMS/ETCS–Class 1, Sep. 2007.

Wang-Sang Lee (M'13–SM'19) received the B.S. degree from Soongsil University, Seoul, South Korea, in 2004, and the M.S. and Ph.D. degrees in electrical engineering from the Korea Advanced Institute of Science and Technology (KAIST), Daejeon, South Korea, in 2006 and 2013, respectively.

From 2006 to 2010, he was with the Electromagnetic Compatibility Technology Center, Digital Industry Division, Korea Testing Laboratory (KTL), Ansan-si, South Korea, where he was involved in the international standardization for radio frequency identification (RFID) and photovoltaic systems as well as electromagnetic interference (EMI)/EMC analysis, modeling, and measurements for information technology devices. In 2013, he joined the Korea Railroad Research Institute (KRRI), Uiwang-si, South Korea, as a Senior Researcher, where he was involved in the position detection for high-speed railroad systems and microwave heating for low-vibration rapid tunnel excavation system. Since 2014, he has been an Associate Professor with the Department of Electronic Engineering, Gyeongsang National University (GNU), Jinju, South Korea. From 2018 to 2019, he was a Visiting Scholar with the ATHENA Group, Georgia Institute of Technology, Atlanta, GA, USA. His current research interests include near- and far-field wireless power and data communications systems, RF/microwave antenna, circuit, and system design, RFID/Internet-of-Things (IoT) sensors, and EMI/EMC.

Dr. Lee is a member of IEC/ISO JTC1/SC31, KIEES, IEIE, and KSR. He was a recipient of the Best Paper Award at IEEE RFID in 2013, the Kim Choong-Ki Award: EE Top Research Achievement Award by the Department of Electrical Engineering, KAIST, in 2013, the Best Ph.D. Dissertation Award: the Department of Electrical Engineering, KAIST, in 2014, the Young Researcher Award by KIEES in 2017.

Sungsoo Park (S'07–M'12) received the B.S., M.S., and Ph.D. degrees in electrical and electronic engineering from Yonsei University, Seoul, South Korea, in 2006, 2008, and 2012, respectively.

From 2010 to 2011, he was a Visiting Scholar with Purdue University, West Lafayette, IN, USA. From 2012 to 2013, he was a Post-Doctoral Researcher with the Information and Telecommunication Laboratory (ITL), Yonsei University. Since 2013, he has been with the Korea Railroad Research Institute (KRRI), Uiwang-si, South Korea, where he is currently a Senior Researcher. His current research interests include wireless communication for train control system, future railway mobile communication system, mission-critical communications and services, autonomous train control, railway safety, and security.

Jae-Ho Lee (S'07–M'15) received the B.S. and M.S. degrees in electronic engineering from Kwangwoon University, Seoul, South Korea, in 1987 and 1989, respectively, and the Ph.D. degree in mechatronics from Korea University, Seoul, in 2005.

From 1989 to 1995, he joined the Technical Research Center, Danam Industrial Co., Ltd., Anyang, South Korea, where he developed onboard power supply, hybrid IC, and so on. Since 1995, he has been with the Korea Railroad Research Institute (KRRI), Uiwang-si, South Korea, where he is currently a Principal Researcher and the Leader of the Train Control and Communication Research Team, KRRI. He has more than 20 years of experience in the railway industrial field and has developed numerous railway signaling equipment. His current research interests include railroad train control, train autonomous techniques, device-to-device communication, energy-harvesting wireless communication networks, train position detection, and radio frequency identification (RFID).

Manos M. Tentzeris (S'94–M'98–SM'03–F'10) received the Diploma degree *(magna cum laude)* in electrical and computer engineering from the National Technical University of Athens, Athens, Greece, in 1992, and the M.S. and Ph.D. degrees in electrical engineering and computer science from the University of Michigan, Ann Arbor, MI, USA, in 1993 and 1998, respectively.

In 2002, he was a Visiting Professor with the Technical University of Munich, Munich, Germany. In 2009, he was a Visiting Professor with GTRI Ireland, Athlone, Ireland. In 2010, he was a Visiting Professor with LAAS-CNRS, Toulouse, France. He has helped develop academic programs in 3-D/inkjet-printed RF electronics and modules, flexible electronics, origami and morphing electromagnetics, highly integrated/multilayer packaging for RF and wireless applications using ceramic and organic flexible materials, paper-based radio frequency identifications (RFIDs) and sensors, wireless sensors and biosensors, wearable electronics, green electronics, energy harvesting and wireless power transfer, nanotechnology applications in RF, microwave MEMS, and system-on-package-integrated (ultrawideband, multiband, mmW, and conformal) antennas, and heads the Agile Technologies for High-Performance Electromagnetic Novel Applications Research Group, Georgia Institute of Technology, Atlanta, GA, USA (20 researchers). He has served as the Head of the GT-ECE Electromagnetics Technical Interest Group, an Associate Director of the Georgia Electronic Design Center for RFID/Sensors Research, an Associate Director of the Georgia Tech NSF-Packaging Research Center for RF Research, and the Leader of RF/Wireless Packaging Alliance, Atlanta, GA, USA. He is currently a Ken Byers Professor in flexible electronics with the School of Electrical and Computer Engineering, Georgia Institute of Technology. He has authored more than 650 papers in refereed journals and conference proceedings, 5 books, and 25 book chapters. He holds 14 patents.

Dr. Tentzeris is a member of the URSI-Commission D, the MTT-15 Committee, and the Technical Chamber of Greece, an Associate Member of EuMA, and a fellow of the Electromagnetic Academy. He was a recipient or corecipient of the 2017 Georgia Tech Outstanding Achievement in Research Program Development Award, the 2017 Archimedes IP Salon Gold Medal, the 2016 Bell Labs Award Competition 3rd Prize, the 2015 IET Microwaves, Antennas and Propagation Premium Award, the 2014 Georgia Tech ECE Distinguished Faculty Achievement Award, the 2014 IEEE RFID-TA Best Student Paper Award, the 2013 IET Microwaves, Antennas and Propagation Premium Award, the 2012 FiDiPro Award in Finland, the iCMG Architecture Award of Excellence, the 2010 IEEE Antennas and Propagation Society Piergiorgio L. E. Uslenghi Letters Prize Paper Award, the 2011 International Workshop on Structural Health Monitoring Best Student Paper Award, the 2010 Georgia Tech Senior Faculty Outstanding Undergraduate Research Mentor Award, the 2009 IEEE Transactions on Components and Packaging Technologies Best Paper Award, the 2009 E.T.S. Walton Award from the Irish Science Foundation, the 2007 IEEE APS Symposium Best Student Paper Award, the 2007 IEEE IMS Third Best Student Paper Award, the 2007 ISAP 2007 Poster Presentation Award, the 2006 IEEE MTT Outstanding Young Engineer Award, the 2006 Asian–Pacific Microwave Conference Award, the 2004 IEEE Transactions on Advanced Packaging Commendable Paper Award, the 2003 NASA Godfrey Art Anzic Collaborative Distinguished Publication Award, the 2003 IBC International Educator of the Year Award, the 2003 IEEE CPMT Outstanding Young Engineer Award, the 2002 International Conference on Microwave and Millimeter-Wave Technology Best Paper Award, Beijing, China, the 2002 Georgia Tech-ECE Outstanding Junior Faculty Award, the 2001 ACES Conference Best Paper Award, the 2000 NSF CAREER Award, and the 1997 Best Paper Award from the International Hybrid Microelectronics and Packaging Society. He was the Chair of the 2005 IEEE CEM-TD Workshop and the TPC Chair of the IEEE MTT-S IMS 2008 Symposium. He is the Vice Chair of the RF Technical Committee (TC16) of the IEEE CPMT Society. He is the Founder and the Chair of the RFID Technical Committee (TC24) of the IEEE MTT-S and the Secretary/Treasurer of the IEEE C-RFID. He is an Associate Editor of the IEEE TRANSACTIONS ON MICROWAVE THEORY AND TECHNIQUES, the IEEE TRANSACTIONS ON ADVANCED PACKAGING, and the *International Journal on Antennas and Propagation*. He served as the IEEE MTT-S Distinguished Microwave Lecturer from 2010 to 2012 and the IEEE CRFID Distinguished Lecturer. He has given more than 100 invited talks to various universities and companies all over the world.